

RICE Infrared Technologies for Environmental Sensing: Present and Future Opportunities and Challenges

F.K. Tittel, R.F. Curl, L. Dong, J. Doty, A.A. Kosterev, R. Lewicki, and D. Thomazy
 Rice Quantum Institute, Rice University, Houston, TX, USA
<http://ece.rice.edu/lasersci/>

OUTLINE

MEMS Alliance Symposium

Washington, D.C.

May 28, 2009

- Motivation: Chemical Sensing Applications
- Fundamentals of Laser Absorption Spectroscopy
- New Laser Sensing Technologies (QEPAS)
- Selected Applications of Trace Gas Detection
 - Quartz Enhanced Photoacoustic Spectroscopy (QEPAS)
 - NH₃ Detection for Environmental Applications
 - Nitric Oxide Detection (LAS & Faraday Rotation Spectroscopy)
 - Monitoring of Broadband Absorbers
- Future Directions of Laser based Gas Sensor Technology

Work supported by NSF ERC MIRTIE, NASA-JSC, DOE STTR and the Welch Foundation

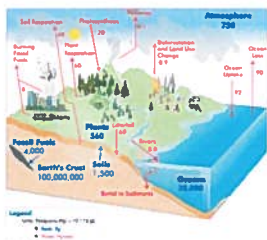
Wide Range of Trace Gas Sensing Applications

- Urban and Industrial Emission Measurements**
 - Industrial Plants
 - Combustion Sources and Processes (e.g. fire detection)
 - Automobile, Truck, Aircraft and Marine Emissions
- Rural Emission Measurements**
 - Agriculture & Forestry, Livestock
- Environmental Monitoring**
 - Atmospheric Chemistry
 - Volcanic Emissions
- Chemical Analysis and Industrial Process Control**
 - Petrochemical, Semiconductor, Nuclear Safeguards, Pharmaceutical, Metals Processing, Food & Beverage Industries
- Spacecraft and Planetary Surface Monitoring**
 - Crew Health Maintenance & Life Support
- Applications in Biomedical and the Life Sciences
- Technologies for Law Enforcement and National Security
- Fundamental Science and Photochemistry

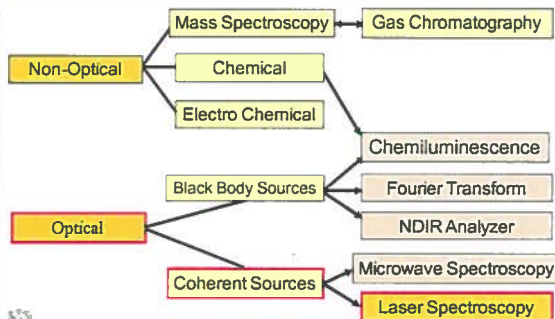


Greenhouse Gases and Climate Change

- Kyoto Protocol Dec. 1997 and Copenhagen Dec. 2009
 - Carbon credit and carbon trading
- Need to measure and locate all sources and sinks
 - Must be in real time and continuous
- Multiple greenhouse gases
 - Carbon dioxide
 - Methane
 - Nitrous oxide



Existing Methods for Trace Gas Detection



Basics of Optical Trace Gas Analyzers



Bear-Lambert's Law of Linear Absorption

$$I(\nu) = I_0 e^{-\alpha(\nu) P_s L}$$

$\alpha(\nu)$ - absorption coefficient [$\text{cm}^{-1} \text{atm}^{-1}$], L - path length [cm]

ν - frequency [cm^{-1}], P_s - partial pressure [atm]

$$a(\nu) = C \cdot S(T) \cdot g(\nu - \nu_0)$$

C - total number of molecules of absorbing gas/ $\text{atm} \cdot \text{cm}^3$ [molecule $\text{cm}^{-3} \text{atm}^{-1}$]

S - molecular line intensity [cm molecule⁻¹]

$g(\nu - \nu_0)$ - normalized spectral lineshape function [cm], (Gaussian, Lorentzian, Voigt)

Key Requirements: Sensitivity, specificity, rapid data acquisition and multi-species detection

Optimum Molecular Absorbing Transition

- NIR Overtones or Combination Bands
- MIR Fundamental Absorption Bands

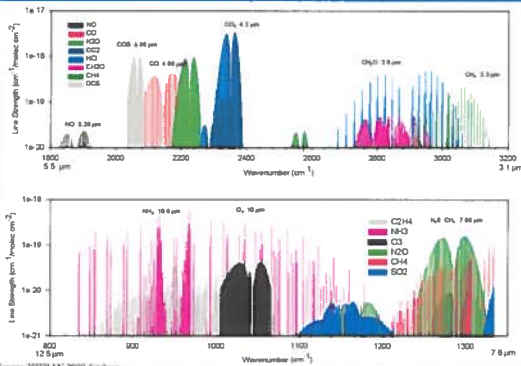
Lens-Optical Pathlengths

- Multipass Absorption Cell (White, Herriott)
- Cavity Enhanced, Cavity Ringdown & Intracavity Spectroscopy
- Open Path Monitoring (with retro-reflector), Standoff and Remote Detection
- Fiber optic evanescent wave Spectroscopy

Spectroscopic Detection Schemes

- Wavelength or Frequency Modulation
- Balanced Detection
- Zero-air Subtraction
- Photoacoustic Spectroscopy (PAS or QEPAS)
- NICE-OHMS, LIBS and LIF

Molecular Absorption Spectra within two Mid-IR Atmospheric Windows



6

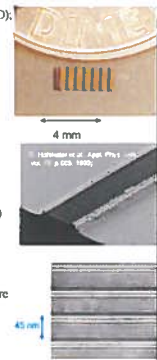
Mid-IR Source Requirements for Laser Spectroscopy

REQUIREMENTS	IR LASER SOURCE
Sensitivity (% to ppt)	Optimum Wavelength, Power
Selectivity (Spectral Resolution)	Single Mode Operation and Narrow Linewidth
Multi-gas Components, Multiple Absorption Lines and Broadband Absorbers	Tunable Wavelength
Directionality or Cavity Mode Matching	Beam Quality
Rapid Data Acquisition	Fast Time Response
Room Temperature Operation	No Consumables
Field deployable	Compact & Robust

7

Key Characteristics of mid-IR QCL and ICL Sources - Nov 2009

- Band – structure engineered devices**
(Emission wavelength is determined by layer thickness – MBE or MOCVD); mid-infrared QCLs operate from 3 to 24 μm (AlInAs/GaInAs)
- Compact, reliable, stable, long lifetime, and commercial availability
- Fabry-Perot (FP), single mode (DFB) and multi-wavelength
- Broad spectral tuning range in the mid-IR**
(4-24 μm for QCLs and 3-5 μm for ICLs and GaSb diodes)
 - 1.5 cm⁻¹ using injection current control for DFB devices
 - 10-20 cm⁻¹ using temperature control for DFB devices
 - > 430 cm⁻¹ using an external grating element and FP chips with heterogeneous cascade active region design; also QCL DFB Array
- Narrow spectral linewidth**
 - CW 0.1 - 3 MHz & <10KHz with frequency stabilization (0.0004 cm⁻¹)
 - Pulsed: ~ 300 MHz
- High pulsed and cw powers of QCLs at TEC/RT temperatures**
 - Pulsed and CW powers of 34 W and 3 W respectively; high temperature operation ~300K
 - >280 mW, TEC CW DFB @ 5 μm
 - > 600 mW (CW FP) @ RT, wall plug efficiency of ~17% at 4 μm.



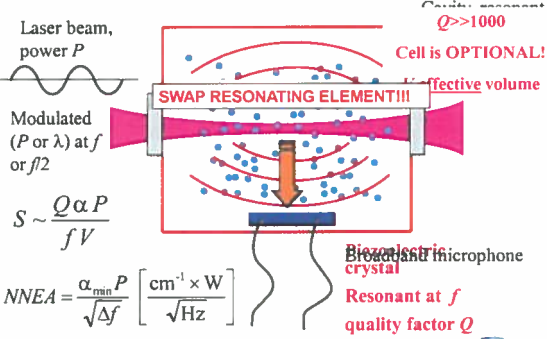
8

Quantum Cascade (QC), Interband (IC) and GaSb Laser Availability in November 2009

- Commercial Sources**
 - Adtech, CA
 - Alpes Lasers, Switzerland & Germany
 - Alcatel-Thales, France
 - Hamamatsu, USA & Japan
 - Maxion Technologies, Inc (Physical Sciences, Inc), MD
 - Nanoplus, Germany
 - Pranalytica, CA
- Research Groups**
 - Harvard University
 - Fraunhofer-IAF, Freiburg, Germany
 - NASA-JPL, Pasadena, CA
 - Naval Research Laboratories, Washington, DC
 - Northwestern University, Evanston, IL
 - Princeton University (MIRTHE), NJ
 - State University of New York
 - Technical University, Zuerich, CH
 - University of Montpellier, France
 - UK: Sheffield


Quartz Enhanced Photoacoustic Spectroscopy

From conventional PAS to QEPAS




$S \sim \frac{Q\alpha P}{fV}$
 $NNEA = \frac{\alpha_{min} P}{\sqrt{\Delta f}} \left[\frac{cm^{-1} \times W}{\sqrt{Hz}} \right]$

Laser beam, power P
 Modulated (P or λ) at f or $f/2$
 Cavity resonant $Q \gg 1000$
 Cell is OPTIONAL!
 Effective volume
 Piezoelectric crystal
 Resonant at f
 quality factor Q

11 

Quartz Tuning Fork as a Resonant Microphone




Unique properties

- Extremely low internal losses:
 - $Q \sim 10,000$ at 1 atm
 - $Q \sim 100,000$ in vacuum
- Acoustic quadrupole geometry
 - Low sensitivity to external sound
- Large dynamic range – linear from thermal noise to breakdown deformation
 - 300K noise: $x \sim 10^{-11}$ cm
 - Breakdown: $x \sim 10^{-2}$ cm
- Wide temperature range: from 1.56K (superfluid helium) to ~700K
- Low cost (<\$1)

Other parameters

- Resonant frequency ~32.8 kHz
- Force constant ~26800 N/m
- Electromechanical coefficient $\sim 7 \times 10^{-6}$ C/m

12 

12

QEPAS spectrophone

$\varnothing 0.41 \text{ mm}$
 Lens
 Excitation laser beam
 10 mm
 3.6 mm
 Quartz tuning fork electrodes

Micro-resonator tubes

- Must be close to QTF but not touch TF (30-50 mm gaps)
- Optimum inner diameter 0.41 mm (10% lower signal with 0.6 mm diameter tubes)
- Each micro-resonator tube ~5mm long (~1/2 for sound at 32.8 kHz)

Gain: $\times 10$ to $\times 20$

Windows

- Must be tilted to prevent reflected light from entering micro-resonator tubes.
- Exact positioning is not important, to the best of our current knowledge.

RICE

QEPAS SNR Enhancement of Acoustic Microresonator

Junction

Microresonator tubes
 Must be close to QTF but not touching (i.e. 30-50µm gaps).
 Each tube is ~5mm long (~1/2 for sound at 32.8 kHz)

QEPAS Signal Gain: $\times 8$ to $\times 20$ depending on pressure & gas

RICE

13

Typical QTF Resonance Curves

$Q = \frac{f_0}{\Delta f_{1/2}}$

— Air, 760 Torr $Q=13\ 270$
 — Vacuum $Q=93\ 500$

TF current, nA

Frequency, Hz

RICE

What about QEPAS Modeling ?

MIRTHE UMBC team: N. Petra, J. Zwick, A. A. Kosterev, S. E. Minkoff and D. Thomazy, "Theoretical Analysis of a Quartz-Enhanced Photoacoustic Spectroscopy Sensor", Appl. Phys B 94, 673-680 (2009)

Also: S. L. Firebaugh, F. Roignant & E. A. Terray, "Modelling the Response of Photoacoustic Gas Sensors", Comsol Conf, Boston, MA, Oct 8-10, 2009

RICE

Alignment-free QEPAS Absorption Detection Module

Resonator tubes, QTF, GRIN lens

RICE

Comparative Sizes of QEPAS & PAS ADMs

Optical multipass cell (100 m):
 $l \sim 70 \text{ cm}$, $V \sim 3000 \text{ cm}^3$

Resonant photoacoustic cell (1000 Hz):
 $l \sim 60 \text{ cm}$, $V \sim 50 \text{ cm}^3$

QEPAS spectrophone:
 $l \sim 1 \text{ cm}$, $V \sim 0.05 \text{ cm}^3$

RICE

18

Merits of QEPAS based Trace Gas Detection

- Very small sensing module and the sample volume (a few mm³)
- Optical detector is not required
- Wide dynamic range
- Rugged transducer – quartz monocrystal; can operate in a wide range of pressures and temperatures
- Immune to environmental acoustic noise, sensitivity is limited by the fundamental thermal TF noise: $k_B T$ energy in the TF symmetric mode, directly observed
- Absence of low-frequency noise: SNR scales as \sqrt{t} , up to $t=3$ hours experimentally verified

QEPAS: some challenges

- Responsivity depends on the speed of sound and molecular energy transfer processes
- Sensitivity scales with laser power

19

WM QEPAS signal for H₂O line @ 7306.75 cm⁻¹, 48 ppmv

Signal, mV rms

Laser current, mA

Signal, $\mu\text{V rms}$

Laser current, mA

$\sigma = 1.6 \mu\text{V}$

Laser power in cell: 9.5 mW; Time constant: 1s; SNR=550
 Peak absorbance: $4.8 \times 10^{-5} \text{ cm}^{-1}$ (HITRAN); RHS: thermal background
 $\Rightarrow \text{NNEA} = 1.9 \times 10^{-9} \text{ cm}^{-1} \text{ W}/(\text{Hz})^{1/2}$; NEC=90 ppbv

20

19

Line locking based on 3f detection

PD

α

P

t

$3f$

21

Principal Architecture of a QEPAS Gas Sensor

Beam Splitter

99%

1%

ADM

Reference Cell

Lock-In Channels

DC 3f 2f

Waveform Synthesis

Σ

DC

Data collection and processing

22

22

Long-term Averaging: H₂S, Allan Variance Analysis

Sigma, ppbv

Time, s

23

QEPAS Performance for 13 Trace Gas Species (Nov. '09)

Molecule (Host)	Frequency, cm ⁻¹	Pressure, Torr	NNEA, cm ⁻¹ W ^{1/2}	Power, mW	NEC (ppbv)
H ₂ O (N ₂)**	7306.73	60	1.9×10^{-9}	9.5	0.09
HCN (air: 50% RH)*	6539.11	60	$< 4.3 \times 10^{-9}$	50	0.16
C ₂ H ₂ (N ₂)	6523.88	720	4.1×10^{-9}	57	0.03
NH ₃ (N ₂)*	6528.36	575	3.1×10^{-9}	60	0.06
C ₂ H ₄ (N ₂)	6177.67	715	5.4×10^{-9}	15	1.7
CH ₄ (N ₂ +1.2% H ₂ O)*	6037.69	760	3.7×10^{-9}	16	0.24
CO ₂ (air+100% RH)	6361.23	150	8.2×10^{-9}	45	40
H ₂ S (N ₂)*	6337.63	780	5.6×10^{-9}	43	5
CO ₂ (N ₂ +1.5% H ₂ O)*	4991.25	50	1.4×10^{-8}	4.4	18
CH ₃ F (N ₂ : 75% RH)*	2804.90	75	8.7×10^{-9}	7.2	0.12
CO (N ₂)	2196.66	50	5.3×10^{-9}	13	0.5
CO (propylene)	2196.66	50	7.4×10^{-9}	6.5	0.14
N ₂ O (air+5% RH)	2193.63	50	1.5×10^{-8}	19	0.07
C ₂ H ₅ OH (N ₂)**	1934.2	770	2.2×10^{-9}	10	90
C ₂ H ₅ F ₂ (N ₂)***	1208.82	770	7.8×10^{-9}	6.6	0.09
NH ₃ (N ₂)*	1046.39	110	1.6×10^{-8}	20	0.066

* Improved microtransducer
 ** Improved microtransducer and double optical pass through ADM
 *** With impulsive modulation and axial microtransducer
 NNEA = normalized noise equivalent absorption coefficient
 NEC = noise equivalent concentration for available laser power and $\tau = 1$ s time constant, 18 dB/dec filter slope

For comparison: conventional PAS 2.1 (2.4) $\times 10^{-9} \text{ cm}^{-1} \text{ W}/(\text{Hz})^{1/2}$ (1,800; 18,300 Hz) for NH₃**

* M. E. Webber et al. Appl. Opt. 42, 2316-2326 (2003). ** J. S. Pilgrimage et al. SPIE Int. Conf. 2007-09-10-13

24